BOLETIN DE LA SOCIEDAD ESPAÑOLA DE
Cerámica y Vidrio
A R T I C U L O

Low temperature synthesis and sintering behaviour of Gd-doped ceria nanosized powders: comparison between two synthesis procedures

V. GIL, J. TARTAJ, C. MOURE

Instituto de Cerámica y Vidrio (CSIC), Electroceramics Department, c/ Kelsen No 5, 28049 – Madrid, Spain.

Two different routes of synthesis of $Ce_{0.9}Gd_{0.1}O_{1.95}$ (CGO) nanopowders are presented; the ethylene glycol-metal nitrate polymerized complex solution method and the precipitation technique using ammonia as the precipitant agent. The powders characteristics were examined by X-ray diffraction (XRD), transmission electron microscopy (TEM), Brunauer-Emmett-Teller (BET) surface area and simultaneous thermogravimetric and differential thermal analysis (TG/DTA). Scanning electron microscopy (SEM) observations were used to determine the agglomeration degree of the powders, and the uniformity of the green compacts. The Hg-porosimetry results were used to investigate the pore size. The densification process was studied by constant heating rate dilatometry and isothermal sintering at different temperatures. Microstructural development of each sample at different sintering temperatures and times was followed by SEM.

Keywords: Ceria, powder processing, sintering, solid electrolyte.

Síntesis y sinterización de polvo nanométrico de ceria dopada con gadolinia: comparación entre dos procedimientos de síntesis

Se presentan dos diferentes rutas de síntesis de nanopolvos de $Ce_{0.9}Gd_{0.1}O_{1.95}$ (CGO): precipitación de hidróxidos, a partir de soluciones de nitratos utilizando amonia como agente precipitante y formación de complejos polimerizados etilene-glicol nitratos metálicos. Las características de los polvos se determinaron por DRX, microscopía de transmisión (TEM), superficie específica por Brunauer-Emmett-Teller (BET), y ensayos de ATD/ATG. El grado de aglomeración de los nanopolvos y la uniformidad de los compactos en verde se ha observado por Microscopía electrónica de barrido, (SEM). El tamaño de poro de los compactos en verde se ha medido mediante porosimetría de Hg. El comportamiento a la sinterización se ha evaluado por dilatometría a velocidad de calentamiento constante y por sinterización isoterma a diferentes temperaturas. La evolución microestructural se ha seguido por SEM.

Palabras clave: ceria, procesamiento de polvo, sinterización, electrolitos sólidos.

1. INTRODUCTION

Solid oxide fuel cell (SOFC) systems have two major advantages, high efficiency and very low emission of pollutants. Up to this date, yttria-stabilized zirconia (YSZ) has been mainly used as the solid oxide electrolyte for such fuel cells because of its good mechanical properties, stability under oxidizing and reducing atmospheres and its nearly pure oxygen ionic conductivity. However, these properties are reached at temperatures over 900ºC and this often leads to reactions between the components, quick thermal degradation of the device and thermal expansion mismatch (1-4). Therefore, it would be desirable to find better oxygen ions conductors than zirconia to reduce operating temperatures of SOFC down to 600-800ºC.

Doped ceria, such as 10 at.% (atomic ratio) Gd or Sm-doped ceria, is an upcoming alternative solid electrolyte against yttria stabilized zirconia (YSZ) in solid oxide fuel cell (SOFC) as a possible application because its higher oxygen ion conductivity and lower interfacial losses with cathode and anode (5-6).

Dense ceramic membranes are needed for electrolytes. However, being a refractory ceramic it is very difficult to achieve dense ceria-based bodies by conventional techniques and without additives at relatively low sintering temperatures (<1500ºC) in air even with long soaking times (7-8). Compromising of the preparation conditions of the ceria with the rest of the SOFC components leads to a poor densification of the ceria electrolyte.

In order to reduce sintering temperatures it would be necessary to obtain non-agglomerated uniform nanopowders. However, due to the high surface energy and chemical activity of the nanoparticles, aggregation and subsequent or simultaneous hard agglomeration are the main difficulties on the way to preparation of these powders. Despite of these problems, recently there have been great efforts in the preparation of highly sinterable ceria-based powders via chemical routes. Among them are the ones based on precipitation techniques (9-11) using ammonia, ammonium carbonate, urea, oxalic acid or hexamethylenetetramine as

precipitant agent. Besides that, there are another preparation techniques including hydrazine preparation method (12), sol-gel processing (13), hydrothermal synthesis (14) and the polymeric organic complex solution method (15-16).

The purpose of this study was to synthesize nanosized $Ce_{0.9}Gd_{0.1}O_{1.95}$ powders for attaining a high degree of densification for ceramic bodies at low temperatures. For this, two different routes were carried out: hydroxide precipitation and a method based on a polymeric organic complex solution. Once obtained both powder types a comparative study of the powder characteristics (agglomeration degree, morphology, size…) and its sintering behaviour by isothermal and constant heating rate dilatometry was carried out.

2. EXPERIMENTAL PROCEDURE

2.1. Preparation of powders

Nanocrystalline $Ce_{0.8}Gd_{0.2}O_{1.95}$ (CGO) powders were synthesized by two different chemical methods. One, a hydroxide precipitation process using ammonia hydroxide as precipitant agent and another, a polymeric organic complex solution method based on a water-soluble alcohol (ethylene-glycol).

In the hydroxide precipitation, the as-prepared transparent solution (0.1 M) consisted of a high purity $Ce(NO_3)_3.6H_2O$ (99.5%, Alfa Aesar) and $Gd(NO_3)_3.6H_2O$ (99.9%, Alfa Aesar), of molar ratio Ce:Gd=0.9:0.1, was heated in air on a hot plate at about 80ºC with magnetic stirring in order to ensure the perfect dissolution and homogenization of the cationic precursors. Lately, the ammonium hydroxide precipitant was added by dropping and blending to the cerium-gadolinium nitrate solution while the mixed solution was continually stirred vigorously. When the precipitation process was completed, a small amount ammonium hydroxide was added in excess so that the pH value was ≈ 9 to precipitate any remaining cerium or gadolinium, which could remain in the solution. After filtering, the precipitate was first washed using distilled water, then several times with pure ethanol (99.5%, Merck) and slowly dried in air at ≈ 80ºC for 24h. These powders will be denoted as HYD in the following.

In the polymeric organic complex solution method, the starting precursor solution was prepared by mixing $Ce(NO_3)_3.6H_2O$ (99.5%, Alfa Aesar) and $Gd(NO_3)_3.6H_2O$ (99.9%, Alfa Aesar), of molar ratio Ce:Gd=0.9:0.1, with 20 ml of distilled water, 80 ml of ethylene glycol and 20 ml of concentrated (60%) nitric acid at room temperature. The as-prepared transparent solution was then heated in air on a hot plate at about 80ºC for 24h with magnetic stirring for the polymerization treatment. Finally, the polymerized solutions were dried at 130ºC for 24h in an oven in air. These powders will be denoted as PCS in the following.

2.2. Characterization of samples

Thermal evolution of the precursors was followed by DTA and TGA techniques, (Netzsch (Germany), model STA-409) incorporating a temperature controller (TASC 414/2 Netzsch). After calcining at temperatures taken according the thermal analysis, and milling, the powders were characterized by X Ray Diffraction with a diffractometer (Siemens D-5000, Erlangen, Germany). The crystallite size (D) of the nanosized powders was calculated using several diffraction lines from the Scherrer formula, $D=0.9\lambda/\beta\cos\theta$, where λ is the wavelength of X-rays, β the corrected half-width that is obtained using the (111) line of the pure silicon as the standard. Specific surface areas of the differently calcined powders were measured by the single-point BET method (Quantachrome MS-16 model, Syosset, NY), using nitrogen as an absorbate after drying under

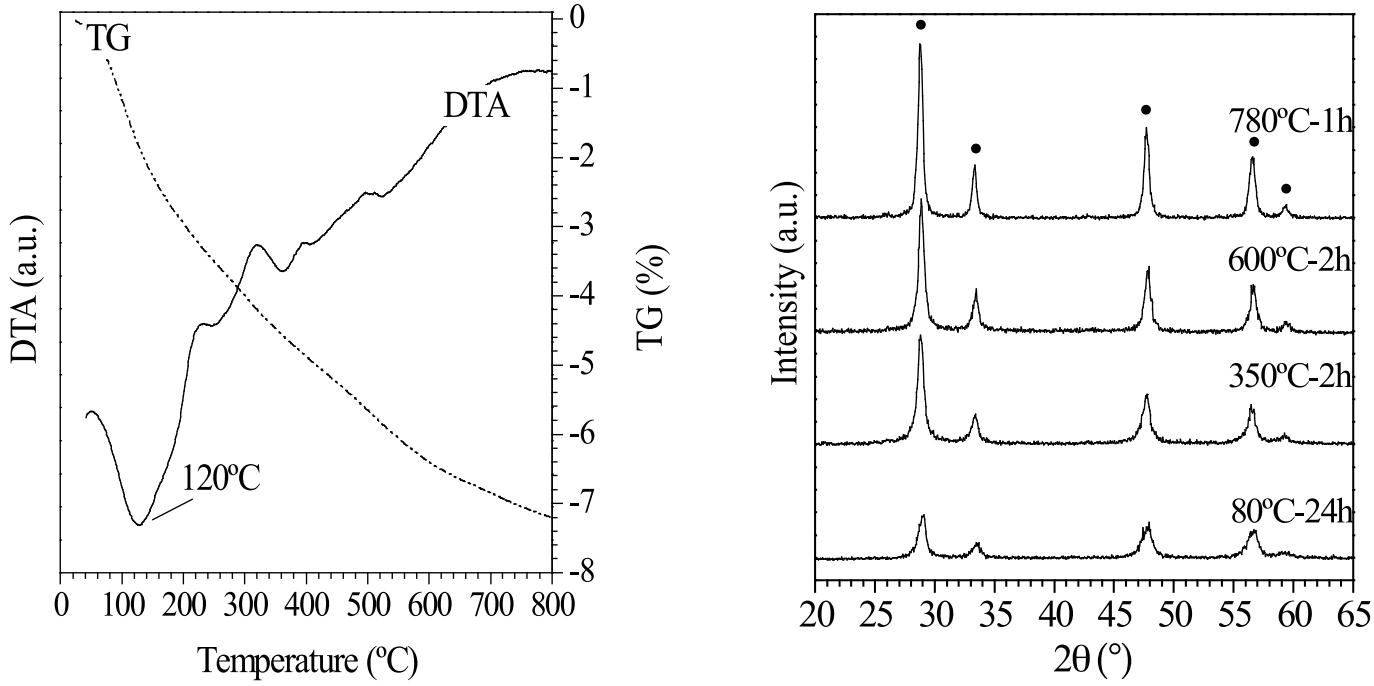

Figure 1. (a) TG/DTA curves between room temperature and 800ºC of powders precursors obtained by precipitation technique; (b) X-ray diffraction pattern after heating-treatment of powders.

vacuum. From the specific surface area data, the particle sizes were also calculated using the equation, $d=6/S*D_{th}$, where d is the average diameter of the assumed spherical particles, S the surface area of the powder, and D_{th} the theoretical density of CGO (~7.24 g/cm^3). The morphology of the calcined powders was studied by SEM (Zeiss DSM 950, Oberkochem, Germany) and TEM, (Hitachi (JAPAN)H-7100 125 kV). Particle size was also measured by Coulter method, (Láser Coulter LS130 Malvern Instruments (U.K.)).

Ball milled and granulated powders were cold isopressed at 200 MPa. Pore size distributions of as pressed compacts were determined by mercury penetration porosimetry (Micromeritics, Autopore II, 9215, Norgross, USA). The samples were sintered in air at a constant rate heating (CRH), using a dilatometer (Netzsch 402E of Geratebau, Bayern, Germany) at a heating rate of 5ºC/min up to 1600ºC. The isothermally sintered samples were heated in the temperature range of 1200º– 1550ºC for 0 to 10 h. Densities were measured by the Archimedes method in water.

The microstructure of sintered samples was examined by scanning electron microscope. The grain size was measured by the line intercept method on the polished and thermally etched sintered samples.

3. RESULTS AND DISCUSSION

3.1. Powder synthesis

3.1.1. PRECIPITATION TECHNIQUE

Figure 1a shows the simultaneous TG/DTA analysis of precipitated powders between room temperature and 800ºC at a heating rate of 5ºC/min. As it can be observed from TG/DTA curves, two well-defined events take place. The first one, an endothermic peak at about 120ºC associated with a weight loss of 1.5% and which might be due to dehydration. The exothermic peaks at the range 250-350ºC suggest that the ceria-gadolinia solid solution suffers a recrystallization step, with growth of particle size, from the previously nanoparticles formed at 80ºC. This low recrystallization temperature indicates an elevated homogeneity and reactivity of the obtained precursors. The weight losses have an end point at temperatures higher than 800ºC, such as is possible to see in the figure 1a.

Figure 1b shows the XRD pattern of the precipitates against heat-treatment temperature. The Miller Indexation was carried out from JCPDS file 75-175. It is noted that the precipitate, simply dried at 80ºC overnight, already presented only peaks corresponding to cubic fluorite structure. The sharp peaks of the precipitates treated at 350ºC for 2h indicate that the crystallization is complete at this temperature, as expected from TG/DTA results. Increasing the calcining temperature enhances particle growth. For eliminating all the volatile components, 600º and 780ºC 2h were chosen to the calcination of precipitates, even taking into account that at 350ºC the fluorite phase is fully formed.

3.1.2. POLYMERIC ORGANIC COMPLEX SOLUTION METHOD

Figure 2a illustrates the simultaneous TG/DTA curves of dried polymeric gel between room temperature and 800ºC at the same heating rate above indicated. From these results it can be supposed that the main residual organic material and volatile elements are not eliminated up to 600ºC.

The TG curve shows two well-defined weight loss steps. In the first one, in a very narrow temperature range, a drastic weight loss of about 40% took place, which is associated in the DTA curve with an abrupt exothermic, very narrow peak, at 180ºC. This indicates that an auto-combustion occurs

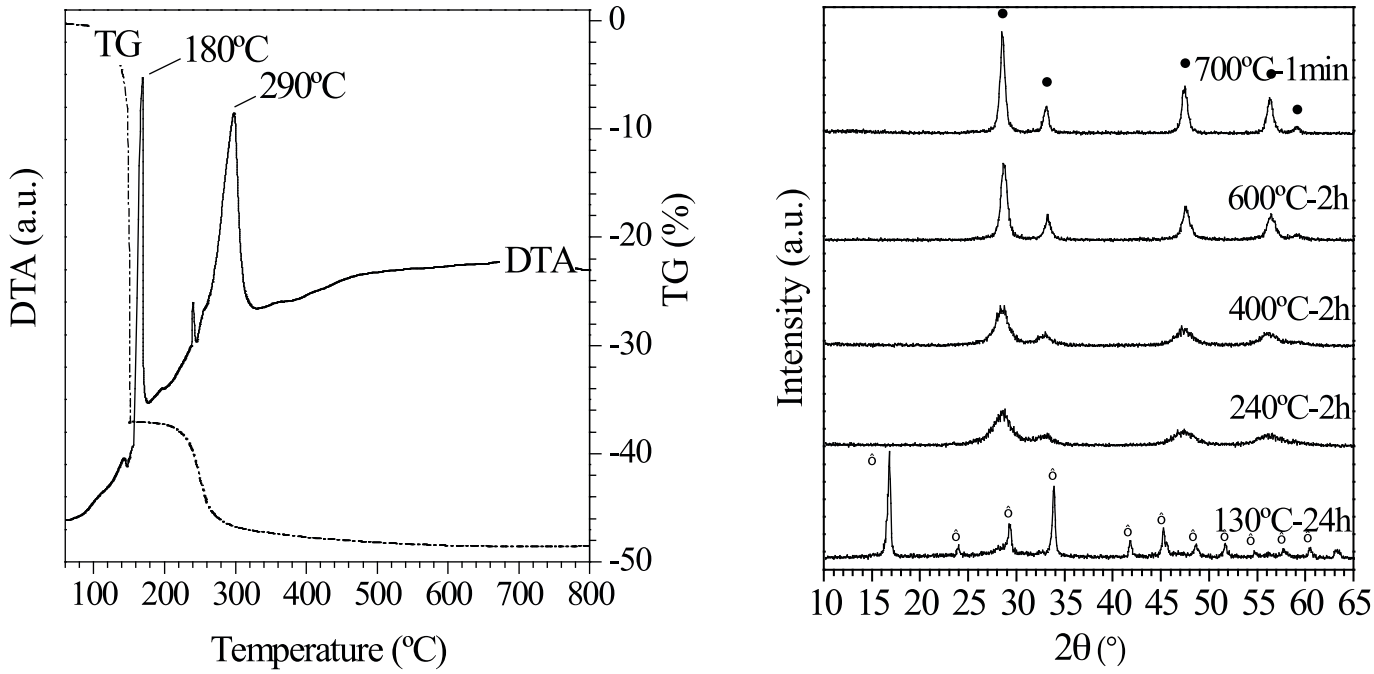

Figure 2. (a) TG/DTA curves between room temperature and 800ºC of powders precursors obtained by PCS-based method; (b) X-ray diffraction pattern after heating-treatment of powders; (•) Fluorite phase: $Ce_{0.9}Gd_{0.1}O_{1.95}$, (™) formate phase: $Ce_{1-x}Gd_x(HCOO)_3$.

during the decomposition of the metal nitrate-ethylene glycol polymerized complex dried gel and, therefore, such a weight loss might be related to the evolution of the carbon compounds as CO_x and nitrogen from nitrates in the form of NO_x. The second one weight loss (~10%) takes place again in a very narrow temperature range, feature related with a weak exothermic peak with its maximum at 230ºC associated with a shoulder at about 260ºC. It was proposed that this is as a consequence of a second auto-combustion. A new and strong exothermic peak at 290ºC is present in the DTA curve, however in this case it may be noted that apparently no weight loss accompanies this last effect. It is therefore inferred that this exothermic peak at 290ºC is due to crystallization, which represents a lower temperature than in the case of precipitation from hydroxides. Nevertheless, temperatures of 600º and 700ºC were chosen for calcining the precursors, thus avoiding possible presence of volatile compounds in the calcined powders.

Figure 2b shows the XRD patterns of the precursor powders treated at 130ºC/24h, 240ºC/2h, 400ºC/2h, 600ºC/2h and 700ºC/1min. XRD analysis demonstrated that the solid intermediate derived from the polymerized solution with a heating time of 24h at 130ºC had XRD patterns consistent with that of well-crystallized cerium-gadolinium formate, $Ce_{1-x}Gd_x(HCOO)_3$, (17), whereas when the polymeric gel was decomposed at 240ºC all diffraction peaks were completely indexed as a cubic fluorite structure. As the temperature treatments increased the enhanced crystallization was observed from the larger and narrower peak intensity.

3.2. Powder characterization

From the precursors prepared from hydroxide precipitation the calcination treatments for obtaining ceramic powders were conducted at 600º and 780ºC for 2 and 1h, and named HYD-6 and HYD-7 respectively; in the case of precursors prepared from PCS, selected temperatures and times were 600º, 2h and 700ºC 1 min, i.e. without time dwell, being 1 min the time for attain temperature; these samples were labeled PCS-6 and PCS-7 respectively. The morphology of the calcined particles is very similar for all of them, such as the Transmission Electron Microscopy, (TEM) show in Figure 3, which shows powder calcined at 600ºC. Table 1 summarizes the main characteristics of the different powders calcined at these different temperatures and times. The CGO powders have a particle size ranging from 15 to 25 nm in all cases, except in the powder obtained from precipitation and calcined at 780ºC (HYD-7) which present a slightly larger particle size (25-35 nm) such as corresponds to this high reactivity conditions. Values obtained from XRD crystallite size measurement and from TEM micrographs are practically the same. In the same way, BET data give also values of size that are in the same magnitude order. The surface areas measured by the BET method were ~38 m^2/g for the powders with higher calcining temperatures and in the case of the powders calcined at 600ºC for 2h (HYD-6 and PCS-6) the BET specific surface areas ranged from about 47 m^2/g up to 56 m^2/g, respectively. On the contrary, Coulter data give higher values of size, which is indicating that there is presence of agglomerates. These agglomerates ranging from 0.5 to 1.0 μm in all cases as it was observed by SEM, Figure 4, with the exception of samples PCS-6 whose agglomeration level increased up to 2 μm. From the results obtained it can be supposed that all the particles are almost spherical and are weakly agglomerated.

Figure 5 shows fracture surface micrographs of compacts obtained by isostatic pressing, in which is possible to see a

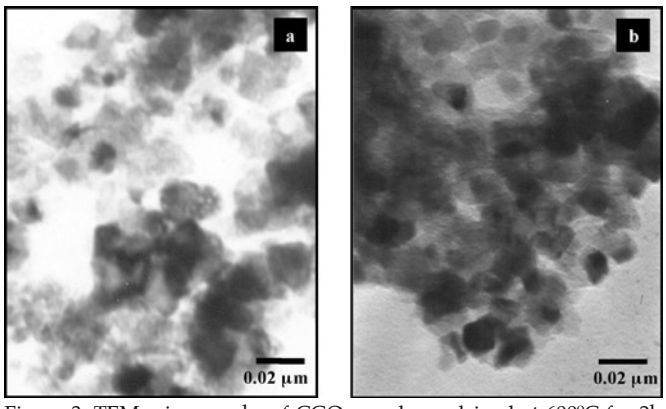

Figure 3. TEM micrographs of CGO powders calcined at 600ºC for 2h and prepared by (a) precipitation and by (b) PCS-based methods respectively.

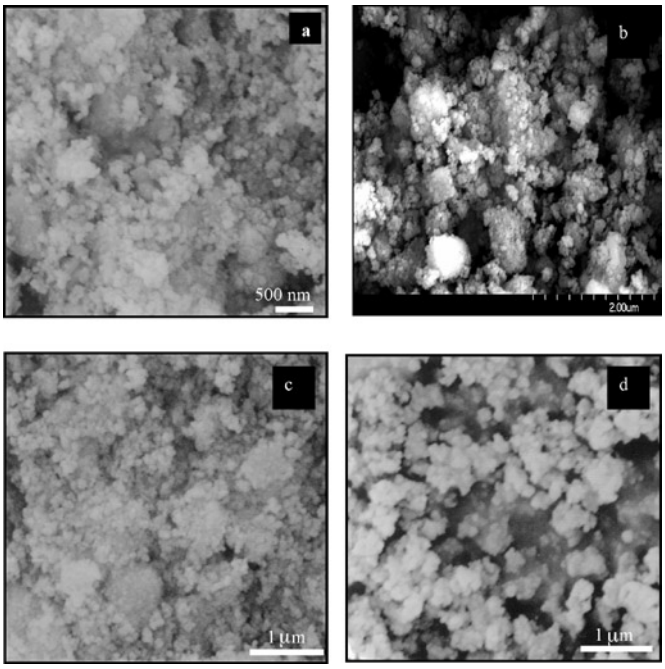

Figure 4. SEM micrographs of CGO powders calcined at different temperatures and prepared by precipitation (a, 600ºC and c, 780ºC) and by PCS-based method (b, 600ºC and d, 700ºC) respectively, showing the agglomerate state.

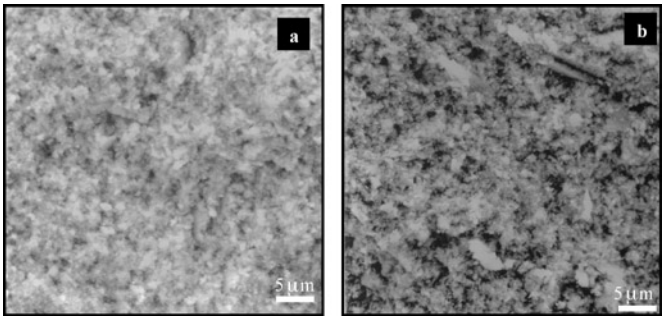

Figure 5.Fracture surface micrographs of compacts obtained by isostatic pressing.

TABLE 1. PHYSICAL PARAMETERS OF CGO CALCINED POWDERS.

Samples	Processing method	Calcining conditions	Particle size, (from BET) (nm)	Particle size, (from XRD) (nm)	Agglomerate size, (from Coulter) (μm)
HYD-6	Precipitation	600ºC-2h	17±1	20±5	0.5-1.0
HYD-7	Precipitation	780ºC-1h	21±1	30±5	0.5-1.0
PCS-6	PCS	600ºC-2h	15±1	20±5	0.5-2.0
PCS-7	PCS	700ºC-1min	25±1	20±5	0.5-1.0

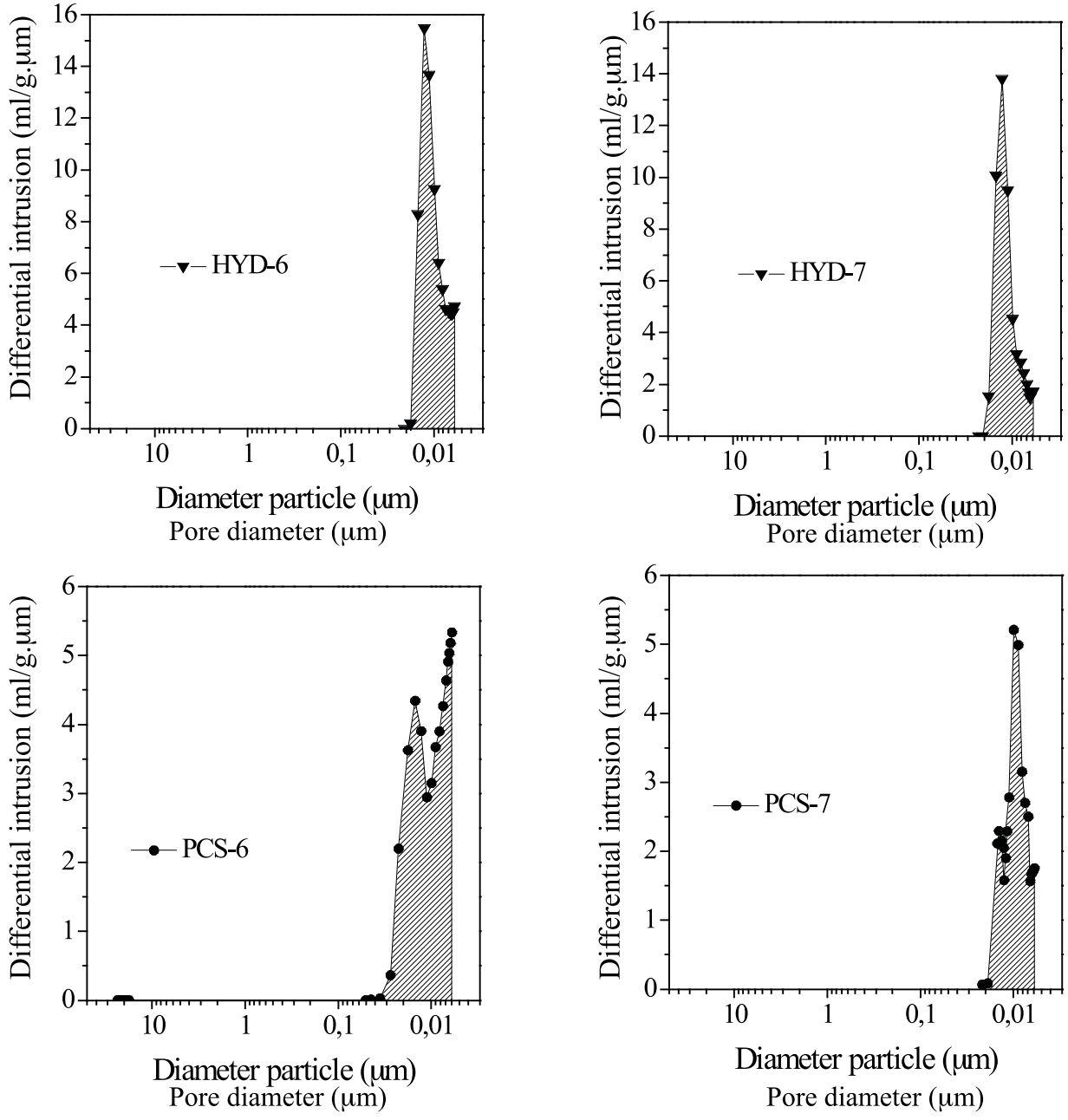

Figure 6. Pore-size distributions of green compacts prepared from CGO powders obtained by precipitation technique and by PCS-based method. Inside the figures are indicated the sample powders.

higher amount of large pores on the surface of PSC sample when compares to the HYD surface. This observation was corroborated by pore size distribution measurements. Figure 6 shows the pore-size distribution curves for the all the green compacts, in which the different types of porosity of the compacts can be appreciated, and are consequence of the different powder characteristics. Thus, the powder with the higher degree of agglomeration shows a wider pore size distribution, Figure 6b. Both PCS powder samples showed two different maxima in the pore size distribution, whereas the HYD powder samples have a narrower, uniform pore size distribution, with a single maximum.

3.3. Sintering behaviour

The differential shrinkage and differential shrinkage rate curves for the different CGO powder compacts measured by dilatometry up to 1600ºC are shown in Figure 7(a-d).

Such as it can be seen the samples prepared from CGO powders obtained by precipitation (Figure 7a and b), show a sintering behaviour that is very similar between them. In these cases the maximum rate of densification takes place at about 1430ºC and the final relative densities at 1600ºC are about 98 and 99% D_{th} for the samples HYD-6 and HYD-7, respectively. Shrinkage is higher for HYD-6, owing to the lower particle size, but the respective curves behaviour shows strong similitude, such as the strong rate shrinkage at 1430ºC and more weak peaks below 1200ºC. In both cases, an end-point shrinkage step can be appreciated below 1500ºC. This similar behaviour in sintering process agrees well with the similitude of the porosimetry curves.

In the case of the CGO powders obtained from PCS (figure 7c and d) it can be observed that those calcined at lower temperature but with a long time, 600ºC/2h, present a sintering behaviour in three steps, with two maxima at 750 and 1060ºC and the one onset at 1600ºC. Such a phenomenon delayed the end point density to a higher temperature (93% of theoretical density, D_{th}, at 1600ºC). However, when the calcining conditions are 700ºC for 1 min, samples with almost full density (99% D_{th}) are achieved and the densification

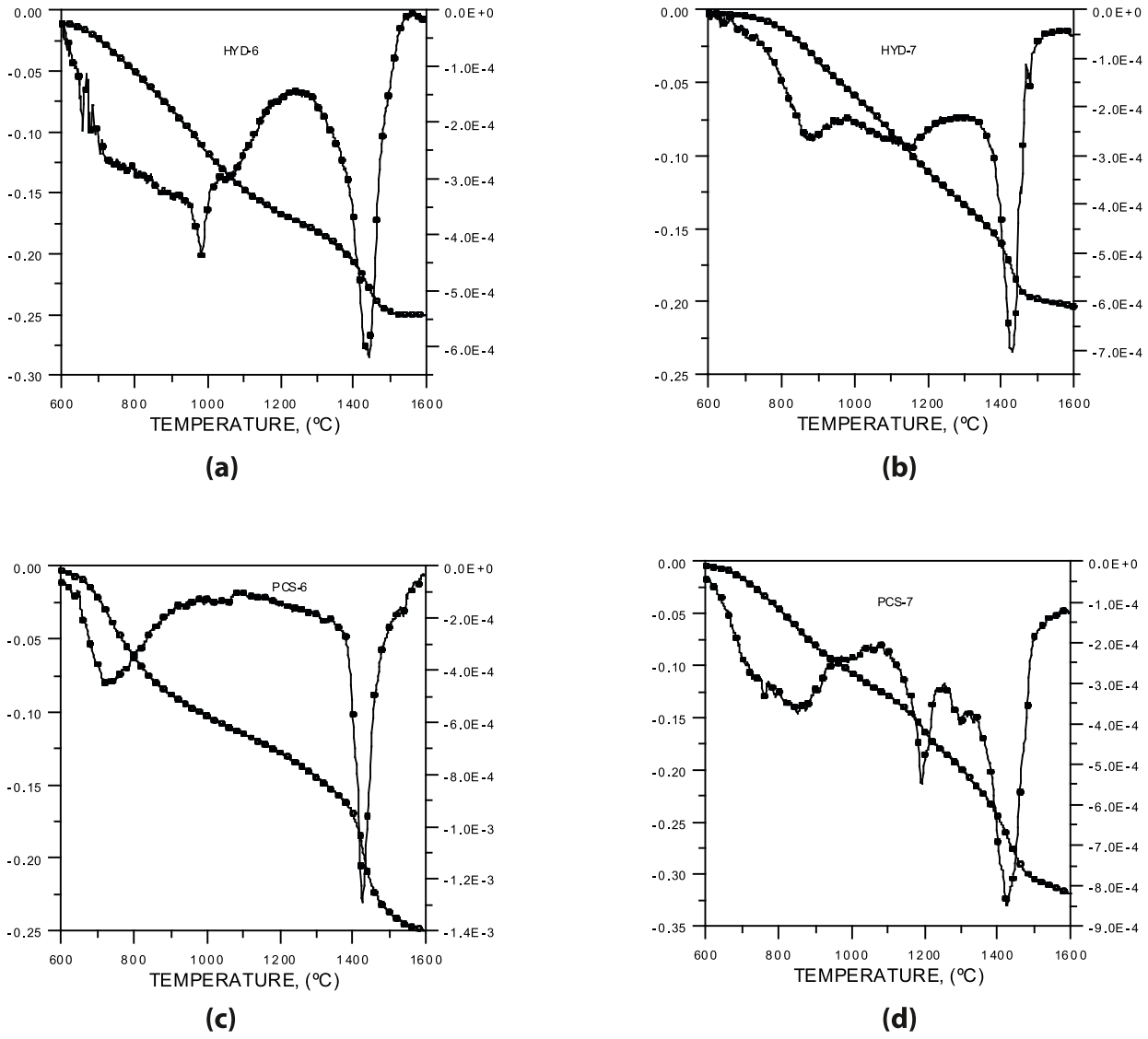

Figure 7. Differential shrinkage and differential shrinkage rate curves for the different CGO powder compacts measured by dilatometry up to 1600ºC; a and b HYD samples, cand d PCS samples.

process takes place only in two steps with a first maximum densification rates at 1200ºC and a second one, more important at 1450ºC, which is a relatively low temperature. Above 1550ºC an end-point shrinkage step seems to take place.

From the above results it can be concluded that the maximum densification rate decreases with increasing both the size of the main pore and the powder agglomeration degree. So, the improved sinterability of the HYD-6, HYD-7 and PCS-7 compacts is strongly related to the lower pore size and the narrower pore size distribution in green compacts, which enhances the driving force for shrinkage of the pores and leads, therefore, to a more rapid and homogeneous densification. The retarding of densification in the case of PCS-6 samples, having the higher agglomeration degree (up to 2m) and a presence of residual porosity with excessively large pores (>10 m) is coincident with the results reported by Roseen et al. (18) that the larger the size of the most frequent pore size in the green compact, the higher the temperature at which these pores are eliminated. From these results it was stated that residual porosity is probably due to the presence of some strong agglomerates, which do not fracture upon pressing.

Figure 8 a y b depict the apparent density against temperature for 4h, and against time, taken at the temperatures of maximum shrinkage rate for each powder type. Sample HYD-7 attains the higher value of apparent density at 1500ºC, 99,5% D_{th} and above this temperature, a dedensification process seems to take place, with a slight fall in the D_{th}. Non-isothermal sintering of the rest of powders led to a less-densified ceramic bodies, being the PSC-7 powder that present a poorer densification behaviour at intermediate temperatures. Isothermal densification at 1430ºC and 1450ºC for HYD-6,7 and PSC-7 respectively shows that the final density is similar for HYD samples, and present a desintering behaviour for times above 5h. The sample PSC-7 needs larger times for attain higher density values. These temperatures are below to those obtained by processing from acrylamide combustion, (19), in which temperatures as high as 1550º-1600ºC were attained, but they are higher than those corresponding to ceramics doped with a third oxide, such as CoO, (20) or Bi_2O_3 (8).

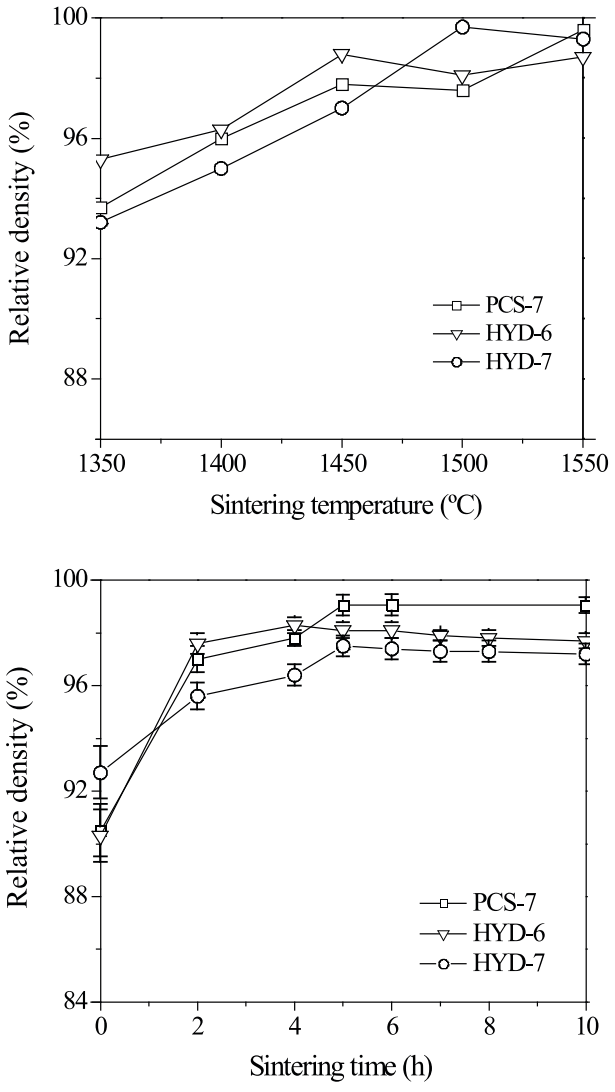

Figure 8. Apparent density (% D_{th}) against temperature for 4h, (a) and against time, (b), taken at the temperatures of maximum shrinkage rate for each powder type.

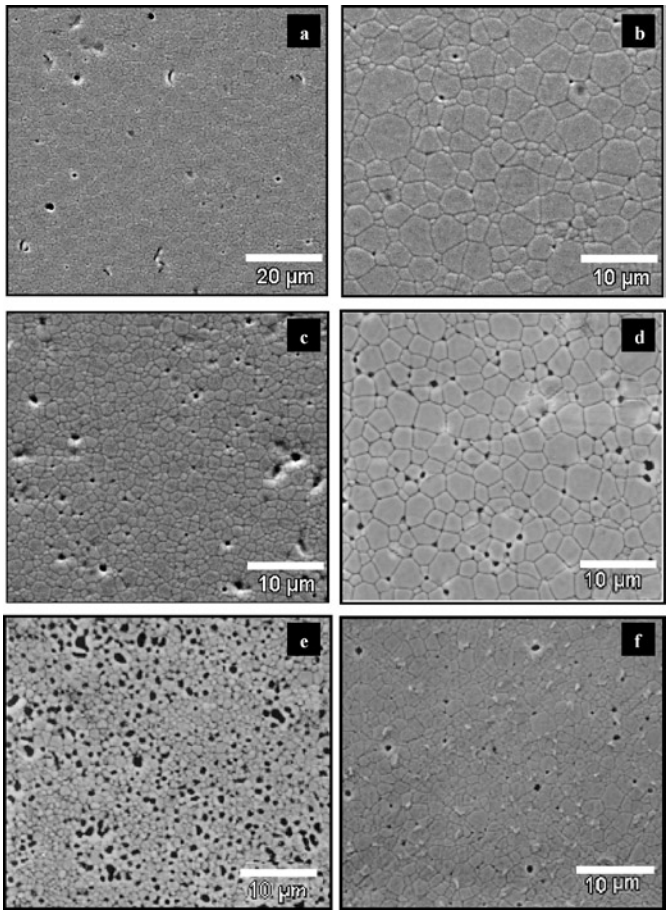

Figure 9. SEM micrographs of polished and thermally etched surfaces of samples (a-b) PCS-7 sintered at 1450ºC and (c-d) HYD-6 and (e-f) HYD-7 sintered at 1430ºC, for 2 and 5h respectively.

3.4. Microstructural development

Figure 9(a-f) shows the microstructural evolution of the CGO samples sintered for 2 and 5h at the maximum densification rate in each case, 1430 and 1450ºC for HYD and PCS samples, respectively. For the samples PCS-7 and HYD-6 apparent densities as high as 97 and 97.6% are attained for only 2h of dwell time. In the case of the HYD-7 at the same sintering conditions only ~95% of the theoretical density is achieved. Near full-density (99.5% D_{th}) is attained for the PCS-7 sample after 5h of dwell time.

With regard to the grain size, this increases with the time sintering from ~4.4±0.6 m to ~5.4±0.8 μm and from ~1.6±0.1 μm to ~3.4±0.3 μm for PCS-7 and CGO-H6 sintered samples, respectively. In the case of the HYD-7 samples a particular feature is been found that is a slower grain growth rate (from ~0.7±0.2 μm to ~1.9±0.3 μm) comparatively with those observed in the rest of the samples, which probably corresponded with different sintering stages.

4. CONCLUSIONS

Both processing methods proposed in this work, ethylene glycol process (PCS) and hydroxides precipitation technique (HYD) lead successfully to obtain weakly agglomerated nanosized CGO powders by means of a low-temperature preparation process. From these powders it is possible to obtain dense bodies with controlled grain growth at significantly lower temperatures that the ones commonly necessary for this material, i.e., 1430-1450ºC vs. 1600ºC. This feature is relevant since a lower sintering temperature minimizes the risk of a possible reduction process (Ce^{4+} to Ce^{3+}) and furthermore it allows a future simultaneous sintering process between electrolyte and electrodes, which would simplify the design and the assembling process of these materials to obtain a fuel cell.

Green compacts having a narrow pore size distribution were compacted as green bodies with the presence of soft agglomerates (HYD-6, HYD-7 and PCS-7), and therefore a homogenous sintering process could take place.

Fine-grained ceramics of CGO with a grain size less than 2.0 μm and a relative density as high as 97.6% can be easily prepared from powders prepared by hydroxides precipitation method, at a sintering temperature of 1430ºC, with a dwell time of 2h. Nearly full-density (99.5%) was achieved in the case of the samples obtained from PCS method (PCS-7) and sintered at 1450ºC for 5h.

ACKNOWLEDGEMENTS

The present work was supported by the Spanish CICYT MAT 2003-01163 Project and a PhD grant from the Autonomous Community of Madrid.

REFERENCES

1. T. Zhang, J.Ma, L. Kong, P. Hing and J. Kilner, Preparation and mechanical properties of dense $Ce_{0.8}Gd_{0.2}O_{2-delta}$ ceramics, Solid Sate Ionics, 167, 191-196, (2004)
2. M. Kamruddin, P. Ajikumar, R. Nihya., A. Tyagi. and B. Raj, Synthesis of nanocrystalline ceria by thermal decomposition and soft-chemistry methods, Scripta Materialia, 50, 417-422, (2004)
3. F. Zhang, S.P. Yang, H.M.Chen and X.B.Yu, Preparation of discrete nanosized ceria powder, Ceramics International, 30, , 997-1002, (2004) .
4. J.S. Lee and S.C.Choi, Crystallization behavior of nanoceria powders by hydrothermal synthesis using a mixture of H_2O_2 and NH_4OH Mater. Lett., 58, , 390-393, (2004)
5. B.C.H Steele., Appraisal of $Ce_{1-y}Gd_yO_{2-y/2}$ electrolytes for IT-SOFC operation at 500ºC, Solid Sate Ionics, 129. 95-110, (2000)
6. M. Godickemeier, K. Sasaki, L.J. Gauckler et al., Electrochemical characteristics of cathodes in solid oxide fuel cells based on ceria electrolytes, Journal of Electrochemical Society, 144,.1635-1646, (1997) .
7. M.A. Panhans. and R.N Blumenthal, A thermodynamic and electrical conductivity study of nonstoichiometric cerium dioxide, Solid State Ionic, , 60, 279-298´(1993)
8. V. Gil, J. Tartaj, C. Moure and P. Durán, Sintering, microstructural development, and electrical properties of gadolinia–doped ceria electrolyte with bismuth oxide as a sintering aid, Journal of the European Ceramic Society, 2006, 26, pp. 3161-3171.
9. Y.M. Chiang, E.B. Lavik and D.A. Blom, Defect thermodynamics and electrical properties of nanocrystalline oxides: Pure and doped CeO_2, Nanostructured Materials, 9, 633-642, (1997)
10. E B Lavik, I Kosacki, H L Tuller, Y-M Chiang and J Y Ying, Nonstoichiometry and electrical conductivity of nanocrystalline CeO_{2-x}, Journal of Electroceramics, 1, 7-14, (1997).
11. K. Higashi, K. Sonoda , H. Ono, S. Sameshima, Y. Hirata, Synthesis and sintering of rare-earth-doped ceria powder by the oxalate coprecipitation method, Journal of Materials Research, 14 957-967, (1999).
12. N. Nakane, T. Tachi , M. Yoshinaka, K. Hirota, O. Yamaguchi, Characterization and sintering of reactive cerium (IV) oxide powders prepared by the hydrazine method, J.Am.Ceram. Soc. 80, 3221-3224, (1997)
13. X. Chu, W.I. Chung and L.D.Schmidt, Sintering of Sol-Gel prepared submicrometer particles studied by transmission electron-microscopy, Journal of the American Ceramic Society, 76, , 2115-2118, (1993) .
14. M. Hirano and E. Kato, Hydrothermal synthesis of nanocrystalline cerium (IV) oxide powders, J. Am. Ceram. Soc. 82 , 786-788, (1999) .
15. S. Wang and K. Maeda, Direct formation of crystalline gadolinium-doped ceria powder via polymerized precursor solution, Journal of the American Ceramic Society, 85, 1750-52, (2002) .
16. P. Duran, F. Capel, D. Gutierrez, J. Tartaj and C. Moure, Cerium IV oxide synthesis and sinterable powders prepared by the polymeric organic complex solution method, Journal of the European Ceramic Society 22, 1711-1721, (2002).
17. S.G Wang, M. Awano, K. Maeda, Low-temperature synthesis of Gd-doped ceria powder by polymerized precursor solutions, J. Ceram. Soc. Japan 110, 703-709, (2002)
18. A. Roosen and H.K. Bowen, Influence of various consolidation techniques on the green microstructure and sintering behaviour of alumina powder, Journal of the American Ceramic Society, 71, 970-977, (1988)
19. S, Piñol, M.Najib, D.M.Bastidas, A.Calleja, X.G.Capdevila, M.Segarra, F.Espiell, J.C.Ruiz-Morales, D.Marrero-Lopez and P.Nuñez, Microstructure conductivity relationship in Gd and Sm doped ceria-based electrolytes prepared by the acrylamide sol-gel related method. J. Solid State Electrochemistry, 8, 650-654, (2004).
20. D. Pérez-Coll, D.Marrero-López, P. Núñez, S. Piñol and J.R. Frade, Grain Boundary Conductivity of $Ce_{0.8}Ln_{0.2}O_{2-\delta}$ Ceramics (Ln=Y, La, Gd, Sm) with and whitout Co-doping, Electrochimica Acta, 51, 6463-6469, (2006).

Recibido: 02-02-09
Aceptado: 26-03-09